THE GEOLOGICAL SOCIETY OF AMERICA

BULLETIN

Volume 115, Number 12, December 2003

ON THE COVER:

Views up a valley on the northern side of the Burhan Budai Shan shortly before the November 14, 2001, Mw 7.8 Kokoxili earthquake. During the Kokoxili earthquake, at least six giant ice avalanches were generated. One ice avalanche comprised >500,000 m3 of ice and snow that moved ~2.7 km beyond the snout of the contemporary glacier at speeds in excess of 20 ms-1 .

Photo by Lewis A. Owen.

See related article : Van der Woerd et al., "Giant, ~M8 earthquake-triggered ice avalanches in the eastern Kunlun Shan, northern Tibet: Characteristics, nature, and dynamics," GSA *Bulletin*, March/April 2004, V.116; no. 3/4, p. 00-00, 14 figures; 2 tables.

Giant, ~M8 earthquake-triggered ice avalanches in the eastern Kunlun Shan, northern Tibet: Characteristics, nature and dynamics

Jerome van der Woerd[†]
Tectonique Active, Institut de Physique du Globe de Strasbourg EOST, 5 rue Rene Descartes, 67084 Strasbourg Cedex, France

Lewis A. Owen[‡]
Department of Earth Sciences, University of California, Riverside, California 92521, USA

Paul Tapponnier
Laboratoire de Tectonique, Institut de Physique du Globe de Paris, 4, Place Jussieu, 75252 Paris Cedex 05, France

Xu Xiwei
China Seismological Bureau, Beijing, China

François Kervyn
Tectonique Active, Institut de Physique du Globe de Strasbourg EOST, 5 rue Rene Descartes, 67084 Strasbourg Cedex, France

Robert C. Finkel
Patrick L. Barnard
Center for Accelerator Mass Spectrometry, Lawrence Livermore National Laboratory, Livermore, California 94550, USA, and *Department of Earth Sciences, University of California, Riverside, California 92521, USA*

ABSTRACT

Several giant ice avalanches were initiated by slope failure from ice caps due to strong ground motion during the 14 November 2001 M_w = 7.9 Kokoxili earthquake on the Kunlun fault. Four ice avalanches were identified on the north slope of the Burhan Budai Shan several kilometers east of the Kunlun Pass, and two were identified on the south slope of the eastern Yuxi Feng, which is ~50 km west of the Kunlun Pass. These ice avalanches originated from steep-sided ice caps and progressed over and past the termini of outlet valley glaciers. In the Burhan Budai Shan, the ice avalanches comprised ice and snow that reached 2–3 km down valley beyond the snouts of the contemporary glaciers. Detailed study of the largest ice avalanche (B2) shows that the initial movement over the contemporary glacier was turbulent in nature, having a velocity >35 ms^{-1}. Beyond the contemporary glacier, the ice avalanche was confined within steep valley walls and entrenched paraglacial fans. Before coming to rest, this ice avalanche moved as a Bingham plastic flow at a velocity of ≤21 ms^{-1}. These ice avalanches transported little rock debris, and it is thus unlikely that they are important in contributing to the landscape evolution of this region. Yet, given the appropriate geologic and climatic conditions, ice avalanching may be an important process in the landscape evolution of high mountainous terrains. The frequency of such events is unknown, but such phenomena may become more common in the future as a consequence of increased glacier and slope instability caused by human-induced climate change. Ice avalanches, therefore, likely constitute a significant geologic hazard in the near future.

Keywords: ice avalanches, earthquakes, glaciers, Kunlun Mountains, Tibet, remote sensing.

INTRODUCTION

The Kokoxili Earthquake, M_w = 7.9 (M_s = 8.1), November 14, 2001 (5:26 pm local time), is the most recent large earthquake to have occurred in northeastern Tibet. It produced an ~400-km-long surface rupture along the Kusai Hu segment of the Kunlun fault between Bukadaban Feng and Burhan Budai Shan (Fig. 1; Xu et al., 2002a, 2002b, 2003; Van der Woerd et al., 2002a, 2003; Dang and Wang, 2002; Lin et al., 2002). Soon after the Kokoxili earthquake, Ikonos high-resolution (January 2002) and Advanced Spaceborne Thermal Emission and Reflection Radiometer (ASTER) satellite images (April 2002) were acquired to identify and map areas of surface rupture. While inspecting these images, six ice avalanches were identified (Figs. 2 and 3). Examination of earlier remote sensing data (e.g., ASTER image of October 2001, Satellite Pour l'Observation de la Terre (SPOT) image of August 1992, and Corona satellite image of September 1968) revealed no evidence of ice avalanches in any of the images taken prior to and during October 2001. Therefore, it was clear that all the ice avalanches must have formed sometime between October 2001 and January 2002. Furthermore, prior to the Kokoxili earthquake, the authors had visited the Burhan Budai Shan on several occasions to undertake tectonic and paleoenvironmental studies. The Xidatan stretch of the Kunlun fault, at the foot of the Burhan Budai Shan, including the fault trace at the outlet of the valley where the largest ice avalanche occurred, was visited in October 2000. The latest visit took place in April 2001. Although there

[†]E-mail: jerome.vanderwoerd@eost.u-strasbg.fr.
[‡]E-mail: lewis.owen@ucr.edu.

GSA Bulletin; March/April 2004; v. 116; no. 3/4; p. 394–406; doi: 10.1130/B25317.1; 14 figures; 2 tables.

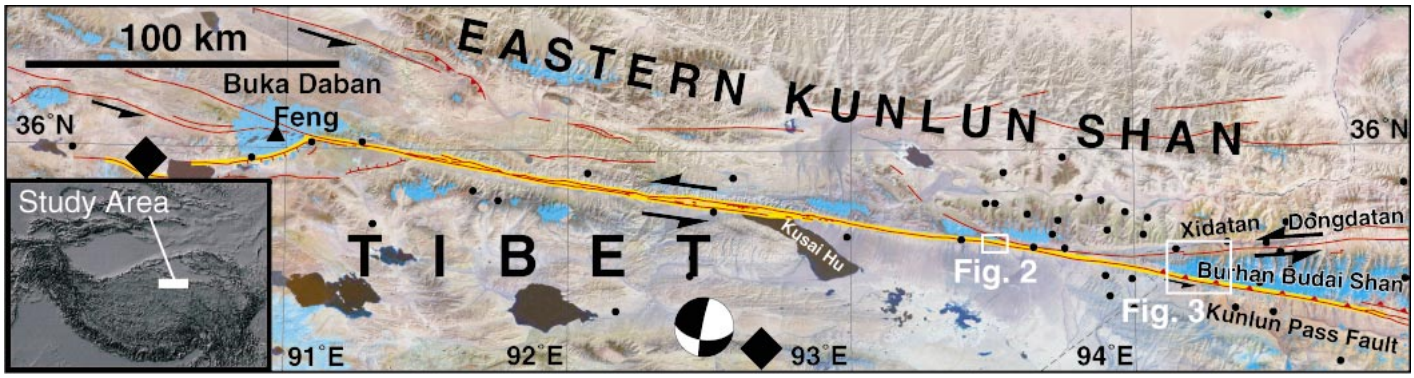

Figure 1. Map of ruptured Kusai Hu segment of Kunlun fault with Landsat image in background (Van der Woerd et al., 2002a, 2002b; Mériaux et al., 2001). Red lines are active faults and yellow lines are ruptured strands. Black diamonds show location of epicenter (west) and centroid with mechanisms (Harvard, 2001) of November 14, 2001 Kokoxili earthquake. Black dots are aftershocks (M≥5). The ice-capped summits appear in light blue, lakes in black. Inset is location of study area within Tibet and rectangles show location for Figures 2 and 3.

is a remote possibility that the ice avalanches are not related to the Kokoxili earthquake, their similar flow characteristics, exceptional size, and the coincidence in timing make it highly likely that they formed as a consequence of strong ground shaking during this large earthquake. Two of these ice avalanches (Table 1, K1 and K2) formed by the collapse of glaciers at the edge of a small ice cap that covers the eastern Yuxi Feng, ~50 km west of the Kunlun Pass, north of the earthquake rupture zone (Fig. 2). The other four ice avalanches (Table 1, B1–B4) originated from collapse of steep sides of the ice cap that covers the northern slope of the Burhan Budai Shan (Shan = Mountain). These ice avalanches progressed 2–3 km beyond the snouts of the outlet glaciers (Fig. 3).

Ice avalanches of this size are rare, and few have been described in detail (Perla, 1980; Alean, 1985; Richardson and Reynolds, 2000; Kääb et al., 2003). The potential hazard from such events was dramatically illustrated on September 20, 2002, when a rock/ice avalanche from the Kolka glacier in the North Ossetian Caucasus in Russia inundated the village of Karmadon, killing >120 people in its path (Kääb et al., 2003). Human-induced global warming and associated environmental changes in the coming decades are likely to increase the frequency of glacial hazards in mountain environments as glaciers continue to melt and thin. Thus, ice avalanches may become more prevalent as slopes become increasingly unstable (Kääb et al., 2003; Bottino et al., 2002). The hazard is further increased in areas of high seismicity. In this paper we describe the characteristics and occurrence of these ice avalanches and document in detail the largest one (B2), which occurred in the Burhan Budai Shan. This will help quantify the dynamics and characteristics and highlight the significance of these hazardous phenomena. Furthermore, we will discuss the implications of such processes for understanding and reconstructing paleoenvironments and landscape evolution in high mountain environments.

REGIONAL SETTING OF THE BURHAN BUDAI SHAN

The Burhan Budai Shan is an east-west-trending, elongated, and wedge-shaped range located in the eastern Kunlun Shan ~120 km south of Golmud (latitude 35.6°N, Fig. 1). The range is ~200 km long, stretching between longitude 94°E and 96°E. The highest summit, the Yuzhu Feng, reaches 6291 m above sea level (asl) in the west, where the range is ~5–8 km wide and the crest line is ~5500 m asl on average. Toward the east, the range widens to ~15–20 km. This is the highest range in this part of the eastern Kunlun Shan, with other crests to the north and the south being <5500 m asl. The range is asymmetric with summits exhibiting steep southern flanks and longer, gentler sloping valleys to the north (Figs. 1 and 4). The Burhan Budai Shan separates the high Tibet plateau at an average elevation of ~4800 m asl to the south from the lower Xidatan valley to the north (~4000 m asl) (Fig. 4). This asymmetric landscape is a consequence of active faulting on both sides of the range. To the south, the Kunlun Pass fault defines the range front. Though it has a left-lateral slip-component (Kidd and Molnar, 1988), this is an active thrust fault primarily responsible for the high elevation of the range (Van der Woerd et al., 2002b). The Kunlun Pass fault ruptured during the Kokoxili earthquake, extending 70 km east of Kunlun Pass (Fig. 1; Xu et al., 2002a, 2002b, 2003; Van der Woerd et al., 2002a, 2003; Dang and Wang, 2002; Lin et al., 2002). To the north, however, the main strand of the Kunlun fault, more specifically its Xidatan-Dongdatan segment, which offsets Quaternary alluvial fans at the foot of the range, did not rupture during this earthquake. Motion on this fault is mainly left-lateral, although normal faults exist on both sides of the Xidatan and Dongdatan valleys (Van der Woerd et al., 2002b).

The glacier equilibrium line altitude (ELA) in this region is ~5200 m asl (Benn and Owen, 1998; Lehmkuhl et al., 1998). This ELA permits the existence of ~50 km² of ice cap along ~75 km of the crest of the Burhan Budai Shan. This ice cap feeds valley glaciers emerging from the range (Fig. 3; Wang, 1987a). The main concentration of glaciers occurs at ~94.25°E-35.67°N around the highest summit, where an ~25 km² ice cap produces ≤500-m-wide outlet glaciers that reach ~2.5 km in length north and south of the range. These are the longest glaciers of the Burhan Budai Shan. The region's climate is arid to semi-arid with precipitation falling mainly during the Asian summer monsoon season. Precipitation increases from <200 mm/yr below 4700 m asl to ~400 mm/yr on the highest peaks (Wang, 1987b). The average annual air temperatures range from −2 °C at altitudes of ~4700 m asl to <−8 °C on the highest peaks (Wang, 1987b). The contemporary glaciers are of continental interior type (Derbyshire, 1981) with cold basal temperatures (Wang, 1987b). The glaciers that extend from the Burhan Budai Shan ice cap are typical of the ''glaciers with limited debris cover'' that are described by Benn and Owen (2002) and Benn et al.

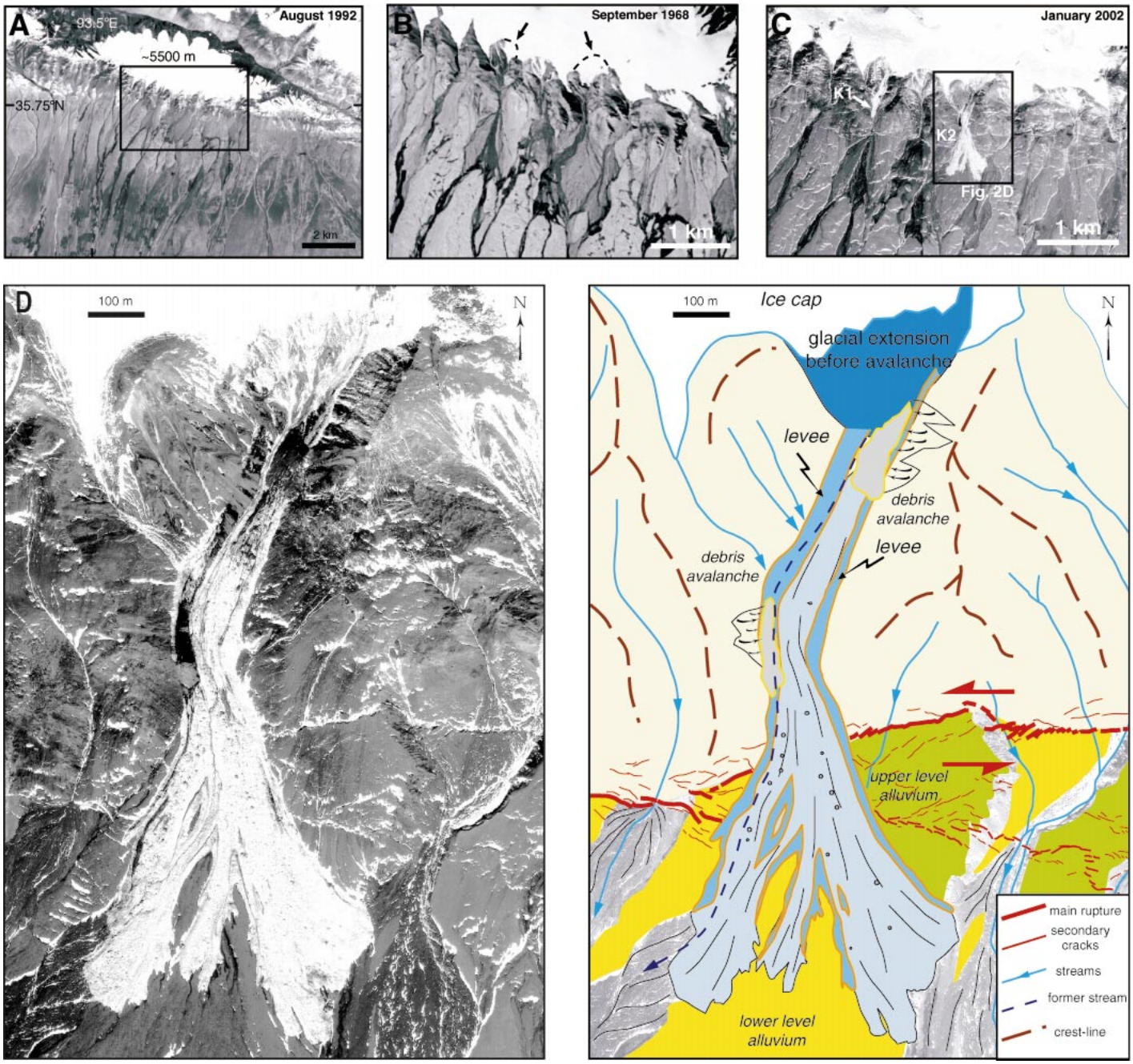

Figure 2. Images of eastern Yuxi ice cap located ~50 km west of Kunlun Pass. This shows the comparisons between SPOT (A), Corona (B), and Ikonos (C and D) images. The dotted lines on (B) indicate areas of the ice cap that failed and formed the two ice avalanches K1 and K2 (C). (D) Detailed interpretation of Ikonos image of ice avalanche K2.

(2003). Glaciation in this region was limited during the last glacial cycle, when glaciers extended less than a few kilometers beyond their present positions (Lehmkuhl et al., 1998; Van der Woerd et al., 2002b).

METHODS

The remote sensing images were first used to map and characterize the form of the ice avalanches and to identify the sources of the ice and snow that fed them. Following the remote sensing analysis, two visits were undertaken to the region (April and May 2002) to examine two of the valleys that contained ice avalanches. Beyond confirming and substantiating the existence of the ice avalanches (Figs. 5 and 6), the fieldwork provided us with an opportunity to examine the characteristics of the transported debris and to make topographic measurements. Although we interviewed local people in the roadside houses and barracks of Xidatan, we were unable to find anyone who had witnessed the ice avalanches occurring or who had any knowledge of their existence or timing. This lack of knowledge of the events may be due, in part, to the difficulty in seeing the ice avalanches, whose termini are several kilometers away from the road and confined within the tribu-

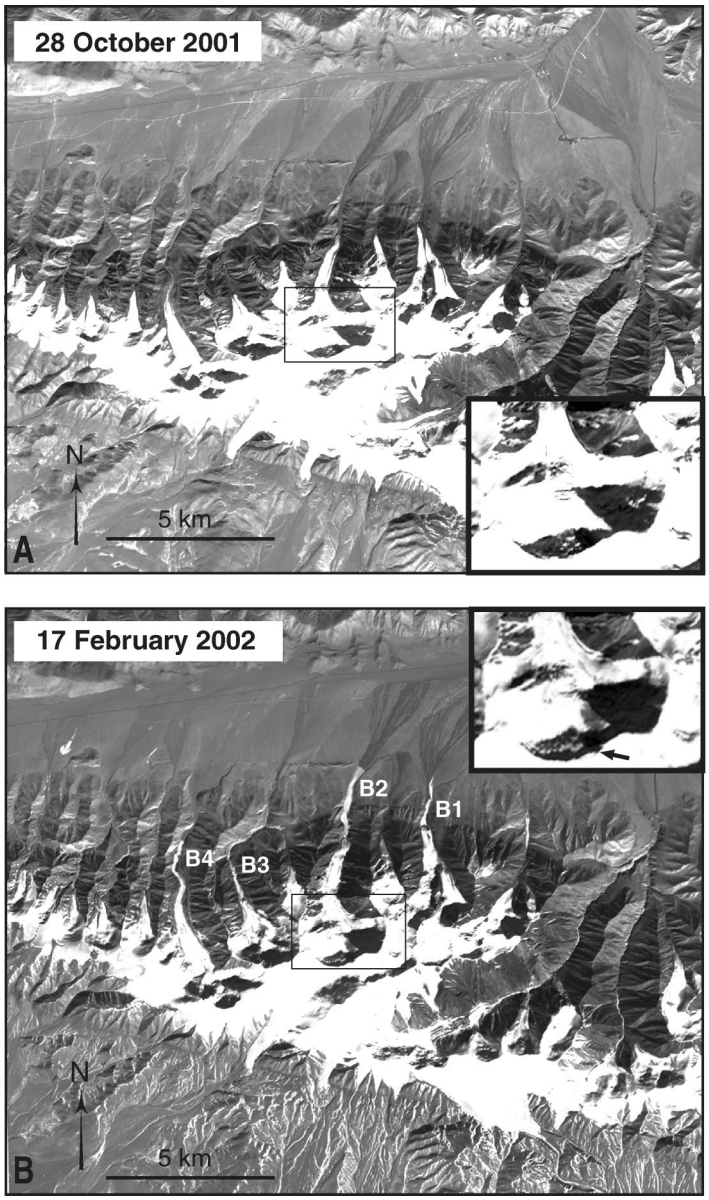

Figure 3. Comparisons between ASTER images of Burhan Budai Shan. (A) Before Kokoxili earthquake (October 2001). (B) After Kokoxili earthquake (February 2002). Images show north-facing glacial cirques with steep valley walls. Insets show enlargement of upper glacial catchment area of ice avalanche B2 and its possible source at steep cliff of ice cap edge (arrow).

TABLE 1. MAIN CHARACTERISTICS OF ICE AVALANCHES ALONG KUNLUN FAULT RUPTURE

Avalanche name	Location		Elevation (m)		Length (m)	Surface (m^2)	Thickness (m)	Volume (10^6 m^3)
	Latitude (°N)	Longitude (°E)	top	bottom				
50 km west of Kunlun Pass								
K1	35.75	93.53	~5200	5100	550	~30,000	~5–10	0.15–0.3
K2	35.75	93.53	~5200	5000	1000	~180,000	~5–10	1–2
Burhan Budai Shan								
B1	35.70	94.28	4480	4355	830	103,027	5–7	0.5–0.7
B2	35.69	94.25	4560	4320	2100	381,510	3–10	1–4
B3	35.68	94.21	~4850	4680	1110	143,100	5–10	0.7–1.5
B4	35.68	94.20	~4750	4520	1950	294,525	3–10	1–4

tary valleys and/or within entrenched streambeds in the alluvial fans.

OBSERVATIONS OF ICE AVALANCHES K1 AND K2

Although these two ice avalanches are remarkably clear on the satellite images, we were not able to visit them in the field (Fig. 2). Both occurred along the south edge of a small ice cap topping the eastern Yuxi Feng at ~93.5°E-35.75N. The Corona (September 1968), SPOT (August 1992), and Ikonos (January 2002) imagery show that these avalanches resulted from the collapse of the lower reaches of two hanging outlet glaciers (Fig. 2). The maximum run-out distance was ~1 km, and estimates of the volumes of snow and ice that were transported are listed in Table 1. The Ikonos image of January 2002 shows that ice avalanche K2 progressed across the fault rupture zone, yet the fault rupture did not disrupt its surface or offset its levees despite the 6–8 m coseismic offset measured in nearby valleys by Xu et al. (2002) (see also Fig. 2D). This demonstrates that the ice avalanche occurred after the Kokoxili earthquake and raises doubts about the alleged 15–16 m total coseismic offset measured by Lin et al. (2002) along one side of glacial avalanche K2 that was incorrectly interpreted as a ''present-day moraine'' (Fig. 2 *in* Lin et al., 2002). In any case, it seems that it is in this area, ~250 km eastward from the epicenter (Fig. 1), that the largest coseismic offsets occurred (Xu et al., 2002), and this, together with east-directed propagation and the correlative buildup of surface wave amplitudes, may explain the occurrence of the giant ice avalanches from here eastward.

ICE AVALANCHES B1–B4

Ice avalanches B1–B4 moved along unnamed valleys and onto the piedmont surface along the northern side of the Burhan Budai Shan (Fig. 3). The valleys are partially filled with glaciers that extend from the Burhan Budai Shan ice cap and contain eroded late glacial moraines and late Pleistocene to Holocene alluvial fans and terraces, which have been well dated (Van der Woerd et al., 1998, 2000, 2002b). Estimates of the size and volume of material involved in each of these ice avalanches are listed in Table 1. The valleys are easily accessible from the Golmud-Lhasa Highway and from the construction sites of the new Golmud-Lhasa railroad.

The topographic maps and images in Figure 7 show the positions, since ~1950, of the two

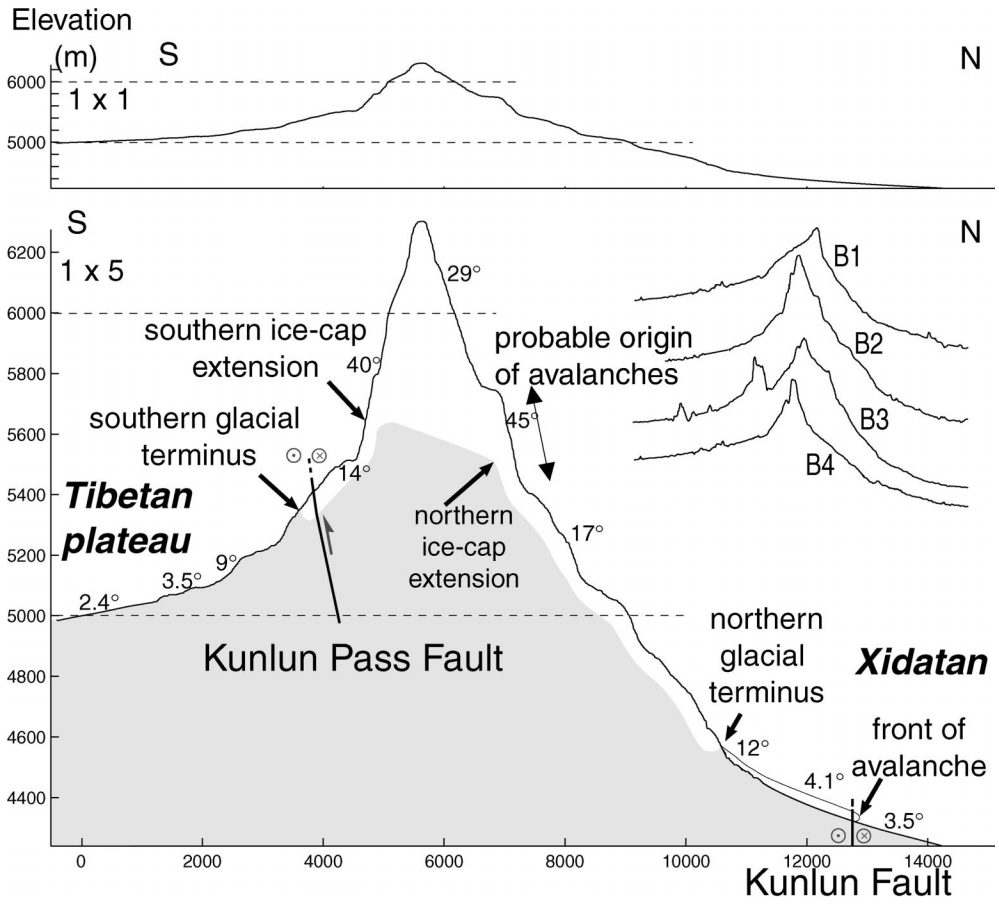

Figure 4. Topographic section for avalanche B2 in Burhan Budai Shan. Asymmetry of north and south slope induces high topographic gradient to north. Average slopes are indicated. Sections for adjacent valleys and glaciers B1, B3, and B4 are comparable.

glacier snouts in the valleys that are now occupied by ice avalanches B1 and B2. The images clearly show that the glacier's snouts have not moved more than a few tens of meters during the last 50 yr, and the glaciers are essentially in equilibrium.

The Ikonos and ASTER images show that ice avalanche B2 moved over the surface of the outlet glacier and proceeded ~2.7 km beyond its snout (Figs. 3 and 8). The avalanche path was confined within the steep-sided valley and apparently followed the west side of the glacier snout, extending beyond the range-front to an altitude of ~4320 m asl. Beyond the range-front, the ice avalanche remained confined within the entrenched alluvial terrace risers. The average slope and total area of the avalanche debris beyond the snout of the glacier are 3–7° and ~381,510 m^2 (Table 1), respectively. The Ikonos image does not cover the probable source area of the avalanche. The ASTER image indicates that the ice avalanche originated from the steep edges of the ice cap (insets of Fig. 3), where slope is steepest (> 40°; Fig. 4).

Using the classification of Alean (1985), the starting zones for the ice avalanches in the Kunlun Shan are of type TII. Such starting zones are places where the glacier or ice cap develops a near-vertical cliff, typically 30–50 m high, as a result of an abrupt longitudinal change in the slope of the glacier's bedrock floor. The ice breaks off when the surface becomes too steep or overhangs. In the case of the Kunlun Shan ice avalanches, our observations suggest that the earthquake-induced ground accelerations initiated failures in areas where the slopes on the ice cap were metastable.

The Ikonos image shows that ice avalanche B2 can be divided into several distinct zones, each of which would have different surface characteristics (Fig. 8). Zone 1, in the lower reaches, consists of jagged blocks of ice and snow that are aligned along longitudinal ridges. Zone 2a comprises smooth longitudinal ridges bounded by high levees that define the margins of the ice avalanche debris. Zone 2b, in the middle reach, is characterized by transverse compressional ridges that rise above the average level of the ice avalanche debris. These transverse ridges offset the longitudinal ridges (this implies that they postdate the avalanche flow; they may be related to an upward-propagating stopping wave). Zone 2c, similar to Zone 2a, contains longitudinal ridges. Zone 3, in the upper reaches of the ice avalanche, is characterized by subsidence of the ice avalanche floor, with wide-open concave upwards cracks. Zone 4 constitutes the starting zone and the contemporary glacier where little ice or debris can be identified.

The field observations confirm that there are distinct zones within the ice avalanche debris. The bulk of the ice avalanche debris rests between its contact with the snout of the contemporary glacier at ~4560 m asl and the ice avalanche terminus at an elevation of ~4320 m asl (Figs. 8 and 9). Apparently, little ice debris remained on the surface of the glacier.

The terminal wall of the ice avalanche in Zone 1 is steep (>30°) and slightly arcuate in plan. It rises more than 10 m above the contemporary floodplain onto which it moved (Figs. 8 and 10). The surface of the ice ava-

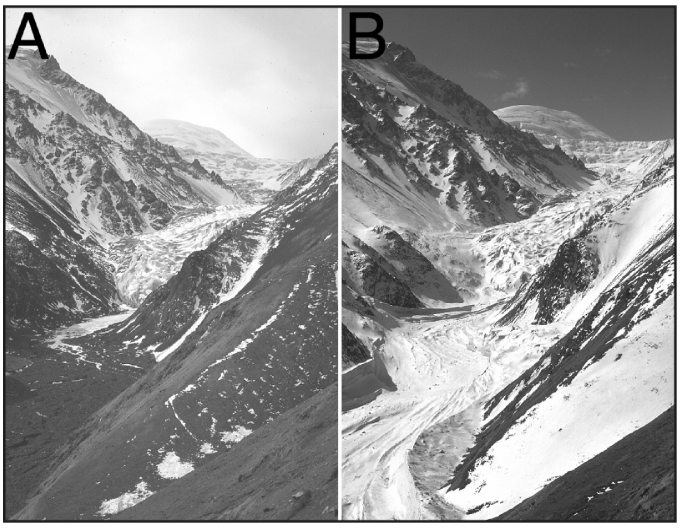

Figure 5. Views (looking south) at snout of glacier in Burhan Budai Shan over which ice avalanche B2 progressed. Images were taken in (A) April 2001 and (B) April 2002.

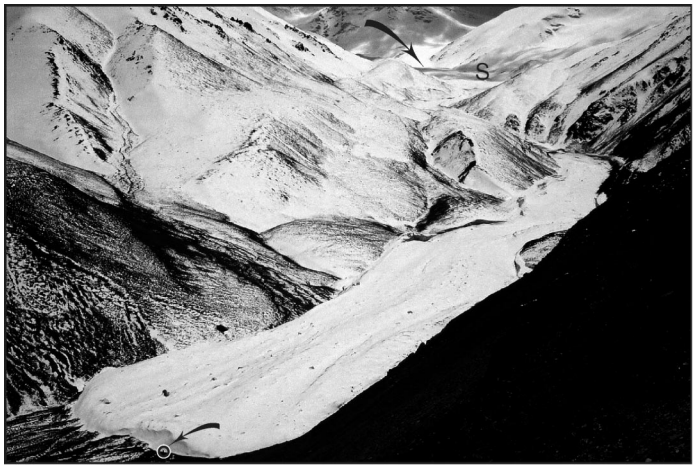

Figure 6. View looking south at ice avalanche B4. Small circle just north of ice avalanche tip surrounds a person for scale. Glacier snout can be seen in valley's upper part (large arrow and S). Photograph was taken in May 2002.

lanche includes jagged, 1- to 5-m-sized blocks of snow and ice that form meter-high pyramids (Fig. 11) arranged in longitudinal rows (Fig. 12). These blocks, analogous to welded breccia, are made of centimeter- to decimeter-sized lumps of glacial ice within a matrix of snow and millimeter-sized fragments of glacial ice (Fig. 11). A millimeter- to centimeter-thick veneer of loose sand and pebble-sized rock fragments, plant, and soil debris is observed sporadically along the surface of the ice avalanche, but little rock debris is observed within the ice avalanche itself, in contrast to what seems to be the case of avalanche K2, for which the color on Ikonos images implies significant mixture of rock and ice. The ice avalanche is higher along its western margin and progressively subsides eastward in 2- to 5-m-high steps spaced several tens of meters apart. The zone with longitudinal ridges stretches ~200 m up valley to an altitude of ~4350 m asl.

Zone 2 of ice avalanche B2 contains a series of relatively smooth longitudinal ridges that stretch over a length of 400 m up to ~4460 m asl. Each ridge has a relief of several meters and is a few tens of meters across (Fig. 13). Levees, composed of ice and snow debris, trace the margins of the ice avalanche and rise up to ~15 m above its surface. The southern margin of this zone is defined by a transverse compressional ridge due to a north-dipping reverse fault (Fig. 13). A series of similar ridges and faults traverses the ice avalanche throughout this zone. As in Zone 1 below, continuous longitudinal ridges exist but are offset by the transverse faults that clearly postdate the longitudinal ridges. Some of the faults are arcuate in form and have concave upward traces (Figs. 8 and 14A).

Above Zone 2b, unfaulted longitudinal ridges extend all the way to the glacier snout at ~4560 m asl in Zones 2c and 3. Very large levees composed of ice and snow rise several tens of meters above the main ice avalanche debris surface (Fig. 14B). The longitudinal ridges meander down this zone (Fig. 9), and the crests of the levees undulate (Fig. 14B). The surface of the ice avalanche becomes progressively lower from the margin to the center of the deposit surface in a series of discrete, meter-high steps (Figs. 9 and 14A).

Comparison of satellite images and field observations indicates that similar structures and flow features characterize the other ice avalanches of Burhan Budai Shan (e.g., Fig. 6, B4), but these ice avalanches were not examined in detail in the field.

ORIGIN AND DYNAMICS OF FAILURE

Although we cannot unequivocally demonstrate that the 14 November 2001 Kokoxili earthquake initiated the ice avalanches in the Kunlun Shan, the long surface rupture (~400 km) and large magnitude of the quake and the east-directed rupture propagation (Kikuchi and Yamanaka, 2001; Rivera et al., 2003; Le Pichon et al., 2003; Bouchon et Vallée, 2003) would have produced strong surface accelerations capable of initiating slope failures, especially in the region where the rupture stopped in the east. Such directivity likely explains why there were no avalanches triggered by the earthquake on the steep slopes of the ice-capped Bukadaban Feng at the western extremity of the rupture. Metastable icefalls and cornices would have been particularly susceptible to failure by avalanching. Furthermore, a significant component of the ice avalanche debris may have been derived from the glacier ice, which would have been capped with firn and fresh snow. The ice avalanches in the Kunlun Shan are exceptionally large, with three exceeding 10^6 m^3 of transported snow and ice. Only eight other ''pure'' ice avalanches are known to have exceeded 10^6 m^3 in historical time. The largest ($2 \pm 1 \times 10^7$ m^3) occurred on Mount Iliamna in Alaska, but it was probably not earthquake-induced (Alean, 1985).

Our field observations of ice avalanche B2

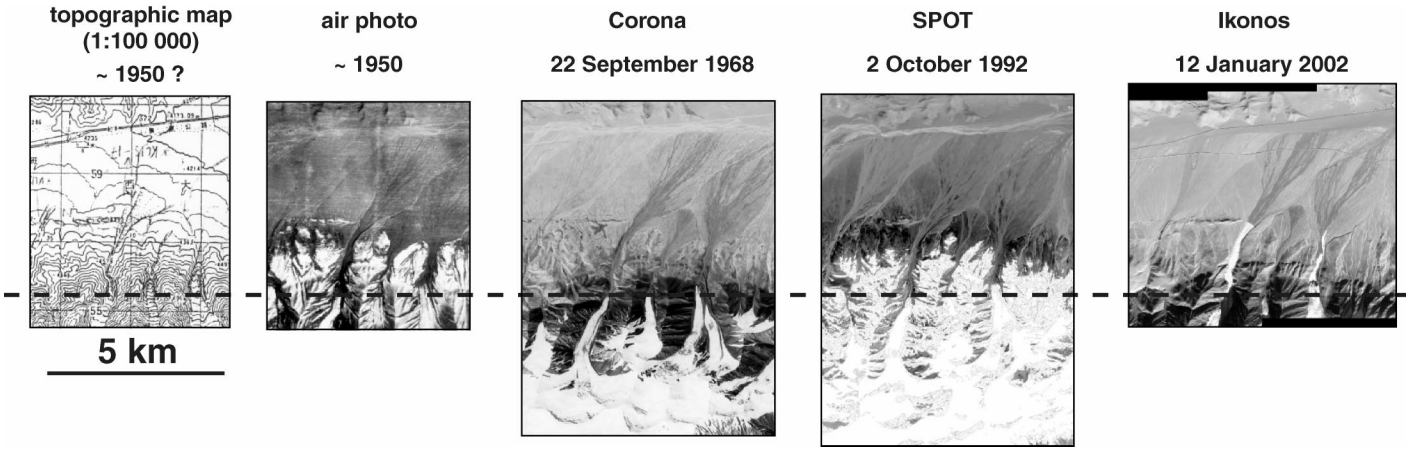

Figure 7. Topographic map and remote sensing images showing positions of glaciers along northern slopes of Burhan Budai Shan for period between 1950 and 2002. Ice avalanches B1 and B2 can be seen on Ikonos image.

yield some insight into the dynamics of failure. The relatively small size of ice blocks within the ice avalanche debris suggests that much of the ice was broken during slope failure and transport. The abundance of snow as a matrix supporting these blocks implies that failure of snow cornices was important. The ASTER image shows a broken crest line just above the glacial cirque that appears to be the most likely source for ice avalanche B2 (Fig. 3B). Unfortunately, given the shape of the valley, this part of the catchment was difficult to see in the field, and our photographs before and after the event yield little additional information. The disintegration of glacial ice into small blocks and its rather chaotic assemblage within larger meter-size discrete blocks suggests that the initial movement over the glacier may have been extremely rapid. The flow was probably turbulent in nature, helping to break the ice into small blocks. Furthermore, the likely absence of ice-avalanche debris over the surface of the glacier supports the view that the velocity of the mass was sufficiently high to have swept most of the debris off and beyond the glacier. The likely distance that the avalanche moved over the glacier was $>$ 500 m (possibly up to 3.5 km). Using case studies and theoretical analysis, Perla (1980) was able to examine the relationships between the vertical drop, path slope angle, run-out distance, volume of debris, and avalanche speed to produce a series of empirical and mathematical relationships between these variables. By means of Perla's analysis, using the run-out distance and volume of the ice avalanche, we estimate that the ice avalanche moved at >35 ms^{-1} (>125 km/hr).

The observations about the deposited ice avalanche material below the glacier, however, are inconsistent with turbulent flow and such high velocities. In particular, the presence of levees and extensive continuous longitudinal ridges are similar to structures observed on debris flows and are more consistent with a Bingham plastic flow (Johnson and Rodine, 1984). None of the typical transverse and concentric ridges characteristic of long run-out landslides (including rock avalanches) that move at extreme velocity, as a combination of turbulent flow, fluidization, and grainflow, are present in the B2 ice avalanche deposit (cf. Rouse, 1984; Erismann and Abele, 2001). Furthermore, the presence of shortening, convex-downward ridges that cross and clearly postdate the longitudinal ridges, suggests that the deposit collapsed and piled up under its own weight as an upward-propagating stopping wave shortly before the debris stopped moving. It is likely that the velocity of the ice avalanche decreased with distance and that the flow became more plastic in nature. This would be particularly likely if the flow contained abundant wet snow and/or was relatively dense. However, it is improbable that wet snow would be present at this altitude in November. Scheiwiller and Hutter (1982) suggested that snow avalanche motion is probably not turbulent in nature because of the increase of friction due to the mutual collision of lumps of compressed snow. Similar effects may hold true for the ice avalanches in the Burhan Budai Shan. Although conversion of gravitational potential energy into frictional heating during movement of the ice avalanche is likely to have produced considerable amounts of water, we did not find any field evidence to suggest significant melting of the ice and snow mass. However, thin, several-decimeter-thick sheets of frozen water more than 10,000 m^2 wide in front of avalanches B1, B3, and up to a meter thick down-valley of B4 (Fig. 3), suggest that some water may have been released from the ice avalanches and was refrozen beyond their limit. Alternatively, this ice may have been the result of dewatering subsequent to the emplacement of the avalanche.

The radial acceleration of the advancing debris forces debris to pile up on outer bends. The velocity of the advancing debris may be estimated by measuring the difference in the heights of levees on either side of the deposit and the radius of curvature along curved reaches. This technique is commonly used to estimate the velocity of debris flows from ancient debris flow deposits (Johnson and Rodine, 1984). Using the equation shown in Table 2, we calculated the velocities for ice avalanche B2. Full analysis of the derivation of this equation is provided in Johnson and Rodine (1984). Our estimates for the velocity of ice avalanche B2 in its middle and lower reaches range from 13 to 21 ms^{-1} ($\sim$47–76 km/hr).

Figure 8. Ikonos image showing main surface characteristics of ice avalanche B2 and an interpretation supplemented with field observations. A, B and C are sections where paleovelocity calculations were performed (see Table 2). Red numbers (1 to 4) refer to zones described in text. Inset enhances part of image remaining in shadow and shows undisturbed glacial tongue terminus.

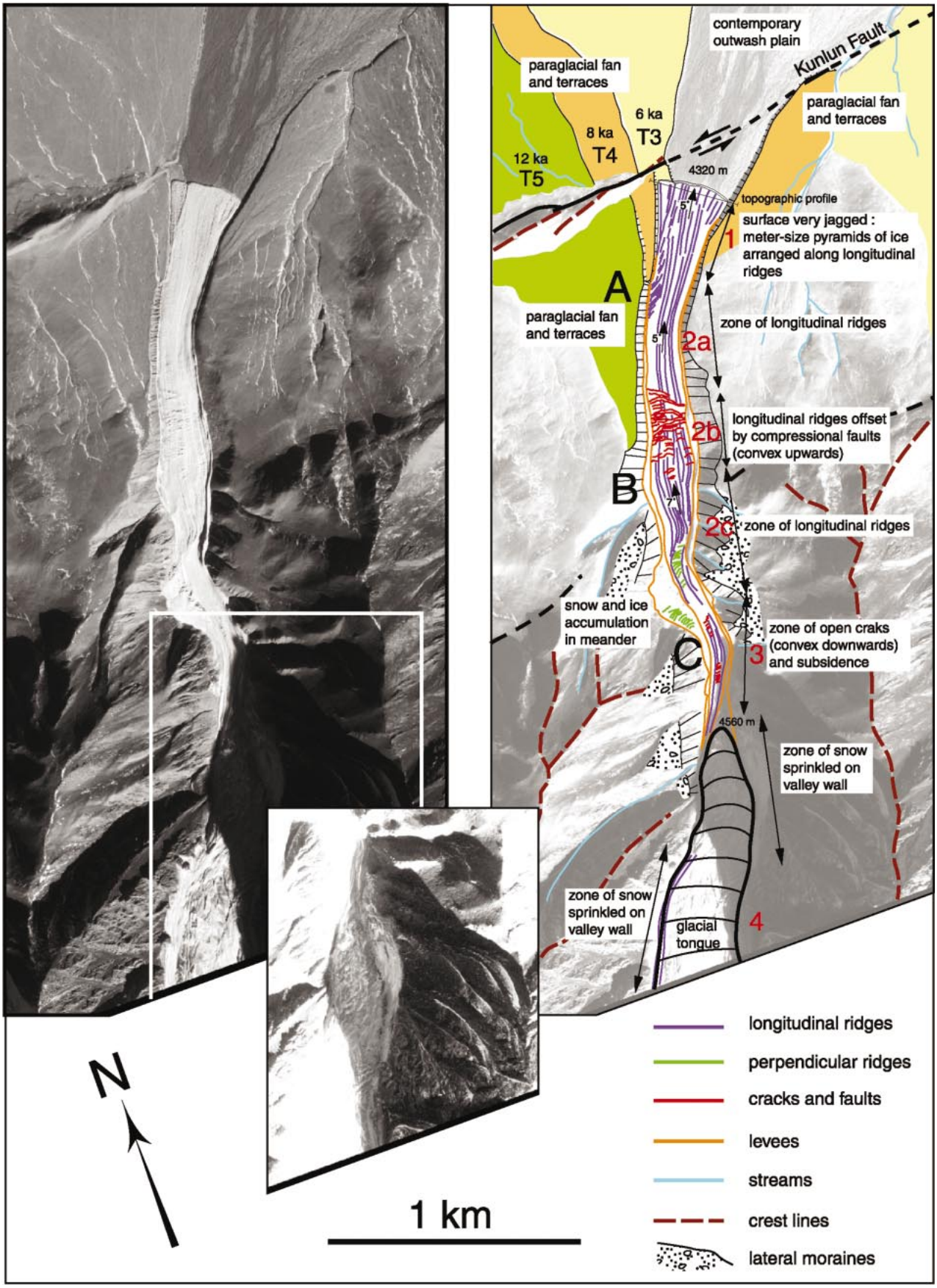
contemporary outwash plain
Kunlun Fault
paraglacial fan and terraces
paraglacial fan and terraces
6 ka
T3
8 ka
T4
12 ka
T5
4320 m
topographic profile
5°
surface very jagged : meter-size pyramids of ice arranged along longitudinal ridges
1
A
paraglacial fan and terraces
zone of longitudinal ridges
5°
2a
longitudinal ridges offset by compressional faults (convex upwards)
2b
B
2c
zone of longitudinal ridges
snow and ice accumulation in meander
zone of open craks (convex downwards) and subsidence
3
C
4560 m
zone of snow sprinkled on valley wall
zone of snow sprinkled on valley wall
glacial tongue
4
N
1 km
longitudinal ridges
perpendicular ridges
cracks and faults
levees
streams
crest lines
lateral moraines

Figure 9. View looking south at glacier and upper and middle run-out zones of ice avalanche B2. Note ~30-m-high levee on east edge of valley. Letter S marks snout of glacier.

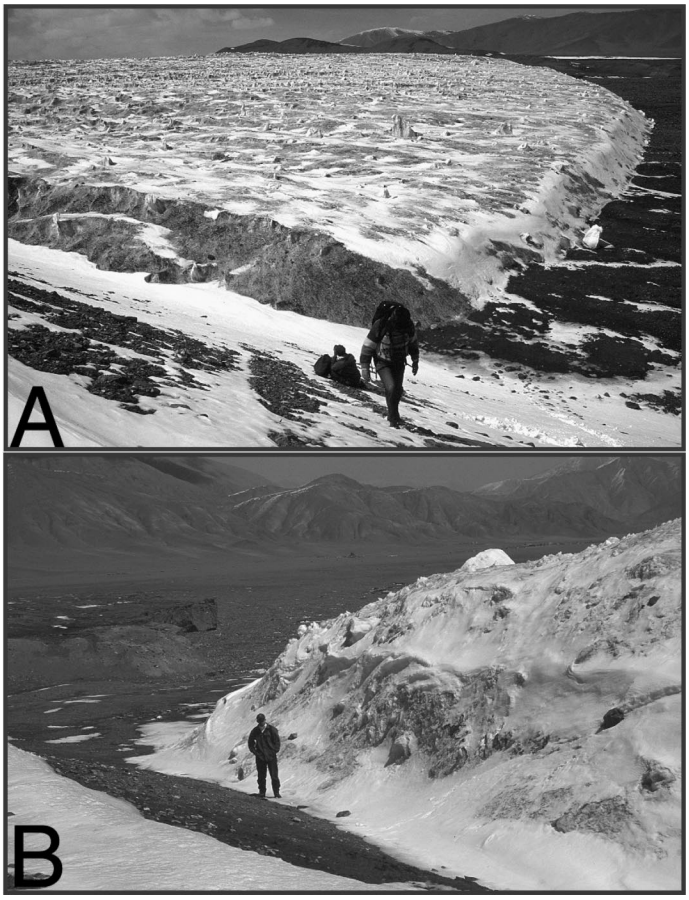

Figure 10. Views of snout of ice avalanche B2 (April 2002). (A) View looking west across snout. Note radiating nature of longitudinal ridges in this zone. (B) Steep front of ice avalanche.

DISCUSSION

Although there are only a few demonstrated cases of ice avalanches triggered by earthquakes, some studies of ice and rock avalanches (Heybrock, 1935; Raap, 1959; Rüegg, 1962; Lliboutry, 1971; Chatellus, 1973; Rothlisberger, 1977; Plafker and Ericksen, 1978; Vivian, 1979; Alean, 1984, 1985; Tufnell, 1984; Evans and Fisher, 1987) provide a basis for comparison. Among these, the Sherman glacier rock avalanche is known to have occurred during the Good Friday, March 27, 1964, earthquake in Alaska (McSaveney, 1978). There are several similarities between that rock avalanche and the ice avalanches in the Kunlun Shan. First, longitudinal ridges formed in the rock avalanche on the Sherman glacier and in the B2, B4, and K2 ice avalanches. Second, the Sherman glacier rock avalanche deposit is made of an assemblage of rock debris in a snow matrix, analogous to the ice blocks in the snow matrix observed in the Kunlun Shan ice avalanches.

McSaveney (1978) suggested that the rock avalanche that spread onto the Sherman glacier was probably a very viscous, complex, fluidized mass of debris, and perhaps a dilatant Bingham plastic that spread like a thin plastic sheet under its own weight. He estimated that the Sherman glacier rock avalanche moved at speeds averaging 26 ms^{-1}, but it reached as much as 67 ms^{-1} in places. This avalanche, however, was not constrained within a valley and between inset terraces. Rather, it progressed onto a glacier where the debris moved as one coherent lobe covering an area of 8.25 km^2. The lobe had a digitate form with debris separated into many long, narrow, curving streams. Ice avalanche K2, which is not confined in its lower reaches, has a similar aspect (Fig. 2D). In contrast, the other Burhan Budai Shan ice avalanches did not divide into distributaries at their distal ends because they were confined within valleys and paraglacial fans.

The catastrophic Nevados Huascaran rock/ice avalanches that occurred in 1962 and 1970 in Peru provide other comparative examples. The 1970 failure was triggered by an earthquake (M~8, 31 May 1970) that resulted in ~50–100 $\times$ 10^6 m^3 of debris advancing down valley, killing an estimated 18,000 people, mainly in the city of Yungay (Plafker and Ericksen, 1978; Chatellus, 1973). The triggering mechanism is unknown for the 1962 avalanche, which resulted in ~4000 fatalities, mostly in the city of Ranrahirca, but the volume of material involved was considerable (~13 $\times$ 10^6 m^3). Both failures were complex, involving ice, snow, rock debris, and vegetation, with velocities averaging ~280 km/hr (~78 ms^{-1}) in 1970 and 170 km/hr (~47 ms^{-1}) in 1962 and reaching total distances of ~16 km from altitudes of between 5400 and 6500 m asl to the Rio Santa at ~2400 m asl. The debris lobes were steep, and abundant

Figure 11. Clasts of glacial ice supported in snow matrix within lower zone of ice avalanche B2.

Figure 12. View south of lower part of ice avalanche B2 showing meter-high pinnacles of snow and ice and a series of longitudinal steps that become progressively lower toward eastern edge of avalanche.

Figure 13. View looking northeast at first transverse compressional structure, cross-cutting longitudinal ridges in middle and lower zones of ice avalanche B2.

rock-impact craters and mud spatters were common.

The Kolka-Karmadon rock/ice avalanche provides another useful comparison. Kääb et al. (2003) describe the combined rock/ice avalanche as having started from a nearly 1.5-km-wide zone between ~3600 and 4200 m elevation on the north face of the Dzimarai-Khokh peak in the Kazbek massif and having fallen onto the Kolka glacier at ~3200 m asl. The impact sheared off part of the Kolka glacier and started a sledge-like rock avalanche of tens of millions of cubic meters. The Kolka rock/ice avalanche crossed the tongue of the Maili glacier and entrained lateral moraines from both glaciers. On the basis of the vertical rise of the rock/ice avalanche as it proceeded around a bend in the valley, Kääb et al. (2003) estimated that the mass moved down valley at ~100 km/hr (~28 ms^{-1}). After ~18 km the rock/ice avalanche came to an abrupt stop and deposited ~80 × 10^6 m^3 of debris. This mass dewatered, resulting in a mudflow up to 300 m wide that traveled for another 15 km down valley.

Unlike the Sherman, Huascaran, and Kolka-Karmadon avalanches, the Kunlun Shan ice avalanches (at least the Burhan Budai Shan avalanches, B1–B4) transported very little rock debris. Such debris was only observed in the lowermost reaches of B2, where it formed small surface patches (a few square meters in extent and a few centimeters thick), constituting a negligible component of the mass and on only one side of B4. It is therefore unlikely that either ice avalanche was effective in transferring much sediment down valley. Both contributed little in reshaping the landscape of the region, in contrast to the Sherman and Huascaran avalanches, which transported huge amounts of debris and reshaped the landscape. We suspect, therefore, that ice avalanches such as those of Burhan Budai might go little noticed in the geologic record, although their contribution to the evolution and transport of the glaciofluvial system can only be fully assessed when their snow and ice has melted completely. However, given the appropriate geologic setting, for example, steep, highly weathered rock slopes and large moraine complexes, significant amounts of debris should be entrained within such ice avalanches. They then become rock/ice avalanches that are common in the geologic record of mountainous regions (Owen, 1991; Fort and Peulvast, 1995; Fort, 2000; Hewitt, 2002; Wieczorek, 2002).

Prior to the emplacement of the ice avalanches, the terraced fan surfaces immediately adjacent to ice avalanche B2 were dated using cosmogenic radionuclide (CRN) techniques

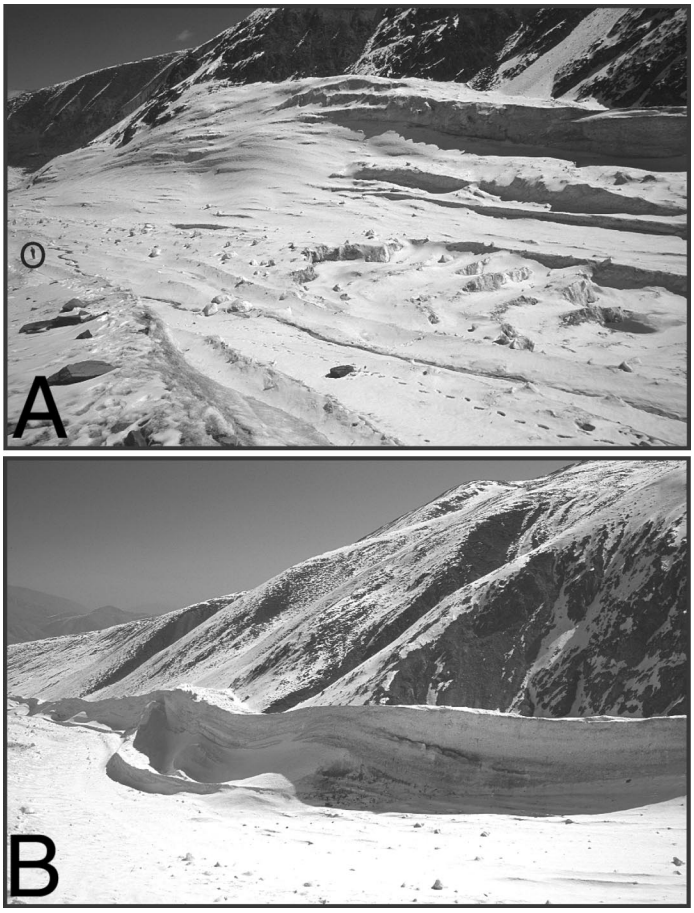

Figure 14. Views of middle zone of ice avalanche B2. (A) View looking northeast across ice avalanche showing trimlines, longitudinal steps, and transverse extensional fractures. Note person for scale (highlighted by the circle). (B) View looking northeast toward undulating levee on eastern side of avalanche.

TABLE 2. ESTIMATIONS FOR VELOCITY OF ICE AVALANCHE B2

Position along avalanche†	Radius of curvature of bend R (m)	Angle of curvature of bend β (°)	Down valley slope α (°)	Velocity v (ms^{-1})‡
A	470–500	3–5	2	15–21
B	215–330	5–7	8	13–20
C	300–330	5–7	6	16–20

†See Figure 8.
‡Velocity estimated using methods of Johnson and Rodine (1984) where $v = g.R.\tan\beta.\cos\alpha$ and G is acceleration due gravity.

(Van der Woerd et al., 1998, 2000, 2002b). Surface pebbles on the three terraces were found to have rather homogenous age clusters ca. 6, 8, and 12 ka (Fig. 8). Such clusters of CRN exposure ages make it unlikely that ice avalanches of this size are recurrent phenomena, carry significant amounts of rock debris, and/or are generally able to override the terrace risers to deposit rock debris onto the adjacent surfaces. Yet, ice avalanche B2, perhaps due to its exceptional downstream reach, did override the lowest of the lateral terraces abandoned 6 ka ago, with risers up to 5 m, and deposited as much as ~5 m of snow and ice on top of it. It will be interesting to quantify the full effect of the ice avalanche once it has melted completely. For now, it appears that the Burhan Budai and K1 and K2 ice avalanches are exceptional events, due perhaps to the coincidence of a very large, rare earthquake and extreme climatic conditions (the post ''Little Ice Age'' warming) that have made the edges of ice caps and hanging glaciers metastable. In Xidatan, the last large earthquake occurred more than 280 ± 90 yr ago (Van der Woerd et al., 1998, 2000). There is now new evidence that the recurrence time of large events on the Kusai segment of the fault is also ~300 yr (Li et al., 2003). If, in fact, the last large events on the fault in the area occurred between 1630 and 1820 A.D., they would have struck during a period possibly cold enough (the Little Ice Age) that no ice avalanche would have been triggered because ice slopes were likely thicker and more continuous and hence probably more stable. Should the current global warming trend continue, however, ice avalanches are likely to become more common in mountainous terrain. Here, the hazard may be especially high. Because of high stress loading on the Xidatan segment of the fault due to slip during the 14 November 2001 earthquake, triggering of another large event on this segment in the years ahead is now much more likely. Though east-directed rupture propagation during this future event might not cause as intense shaking as that induced by the Kokoxili earthquake, one should take into account the fact that the Burhan Budai icecap has likely been greatly weakened and destabilized by that earthquake. Clearly, therefore, the level of hazard awareness in Xidatan, as well as the level of careful geophysical monitoring, should be raised until the next large earthquake strikes.

Ice avalanches of the size described in our paper may have important implications for the glaciological system and for paleoenvironmental reconstructions, particularly when they occur during glacial times. Ball (1875), Benn and Evans (1998), Benn et al. (2003), and Benn and Owen (2002), for example, describe how ice avalanches play important roles in helping to regenerate glaciers in the European Alps and the Himalaya. The ultimate result of such avalanching is a ''reconstituted glacier.'' If large quantities of snow and ice debris become integrated into an advancing glacier, they help extend the glacier to elevations lower than the climatic conditions would normally support. Reconstructions of the former size and equilibrium line altitude (ELA) made from geomorphic evidence left behind by such glaciers would therefore not be representative of the regional climatic conditions. Benn and Lehmkuhl (2000) warned against such effects when they discussed the relevance and difficulties of reconstructing former ELAs in high mountain environments.

The low average annual temperature and aridity of the Burhan Budai–Xidatan–Kunlun region will probably allow the ice avalanches

to last many decades in the valley. Should the contemporary glaciers advance, the avalanches' ice and snow may become assimilated to form reconstituted glaciers. However, because the remote sensing data suggests that the Burhan Budai glaciers are in equilibrium (Fig. 7), and because Su and Shi (2002) have shown that most glaciers of the Tibet Plateau have been retreating since the Little Ice Age, it seems unlikely that the contemporary glaciers will advance in the near future to form reconstituted glaciers.

Unfortunately, the lower preservation potential of pure ice avalanches in the geologic record may account for the importance of ice avalanches as geologic hazards being overlooked. Although we believe that the Kunlun ice avalanches were initiated by seismic activity, similar ice avalanches may be initiated by other factors, such as changes in the glaciologic and climatic regime. Given the likely future climatic instabilities resulting from human activities, the prevalence of ice avalanches may increase in the coming decades as glaciers and slopes adjust to changing environments. There is increasing awareness that the major landscape changes that occur in glaciated terrains take place during times of climatic instability, notably during deglaciation (Ballantyne, 2002; Barnard et al., 2003). During such times, it is likely that the frequency of ice avalanching will increase as glaciers melt and thin and slopes become progressively more unstable. Under these circumstances, ice avalanches become an important factor in the landscape evolution. It is therefore particularly urgent to highlight the importance of recognizing these phenomena as geologic hazards.

CONCLUSIONS

Few giant ice avalanches have been described. This is probably because they are uncommon, rarely leaving a noticeable trace in the geologic record and/or going unnoticed in remote mountain regions. Yet, given the increased use of mountainous regions and possible human-induced climatic instability, ice avalanches are likely to become more common in the near future and may constitute a significant geologic hazard in glaciated mountainous terrains. The Kunlun Shan ice avalanches are among the largest described and help illustrate the characteristics and nature of such events.

The six avalanches we document here were likely initiated by strong ground shaking due to the eastward propagation of the 14 November 2001 Kokoxili earthquake. The Kunlun Shan ice avalanches transported huge volumes of snow and ice down valley (Table 1). The initial motion on top of the glaciers was probably turbulent, with velocities of >35 ms^{-1}. Beyond the glacier snout, the avalanching ice and snow probably slowed to 13–21 ms^{-1} and progressed as a Bingham's plastic flow confined within the steep valley and entrenched paraglacial fans and terraces.

There is little evidence for significant transport of rock within the snow and ice, and thus the Kunlun ice avalanches are probably not primary agents of landscape evolution. Under the right geologic and climatic settings, however, significant debris may be entrained within ice avalanches, and they then become ice/rock avalanches and are important processes for sediment transfer and landscape evolution in mountainous regions. Furthermore, ice avalanching is important for understanding glacier mass balances. Ice and snow deposited by ice avalanches, for example, may become incorporated into advancing glaciers, producing reconstituted glaciers and leading to positive glacier mass balances. In the case of the Kunlun ice avalanches, we are uncertain how long the deposited ice will remain in the valley before it completely melts away. Given the current global warming trend, it is unlikely that the Kunlun glaciers will advance and incorporate the avalanche ice. Nevertheless, the low temperatures and aridity of the region will probably help preserve these landforms for many decades to come. Because of the likelihood of a large, impending earthquake in the Xidatan trough, which is the main road access to northern Tibet, and where the new Golmud-Lhasa railroad is presently under construction, enhanced surveying and continuous monitoring of the steep northern flank of the already destabilized Burhan Budai ice-cap should be implemented at once and maintained for years to come.

ACKNOWLEDGMENTS

We thank Carrie Patterson, Douglas Benn, and Keith Brugger for their constructive and positive reviews of our manuscript. This work was supported by Institut National des Sciences de l'Univers and Centre National de la Recherche Scientifique and by the Lawrence Livermore National Laboratory (LLNL) (under DOE contract W-7405-ENG-48) as part of an Institute of Geophysics and Planetary Physics/LLNL research grant and the Pacific Rim Research Program of the University of California. We particularly thank Philippe Vidal for specific funding and the Ministère des Affaires Etrangères for field support. We thank Y. Klinger, G. King, and D. Bowman for their support in the field and thoughtful discussions. ASTER images are distributed by the Earth Resources Observation Systems (EROS) Data Center Distributed Active Archive Center, located at the U.S. Geological Survey's EROS Data Center in Sioux Falls, South Dakota. This is Institut de Physique du Globe de Strasbourg contribution N° 2003.29- UMR7516.

Note in proof: We visited the region in November 2003, two years after the 14 November 2001 earthquake that caused the avalanches. Unexpectedly, all the avalanches had already melted away except for a few icy patches in the shadows of the valley's flanks. Instead of several decades, as we had forecasted, only two years were enough to almost completely melt the avalanches, despite the high elevation and cold winter temperatures. The rapid disappearance of such volumes of ice and snow emphasizes the importance of remote sensing techniques in high mountainous regions to detect such events and make hazard studies.

REFERENCES CITED

Alean, J., 1984, Ice avalanches and a landslide on Grosser Aletschgletscher: Zeitschrift für Gletscherkunde und Glazialgeologie, v. 20, p. 9–25.

Alean, J., 1985, Ice avalanches: Some empirical information about their formation and reach: Journal of Glaciology, v. 31, p. 324–33.

Ball, J., 1875, Bernese Alps including Oberland (Ball's Alpine Guides): London, Longman and Co., p. 144.

Ballantyne, C.K., 2002, Paraglacial geomorphology: Quaternary Science Reviews, v. 21, p. 1935–2017.

Barnard, P.L., Owen, L.A., and Finkel, R.C., 2003, Style and timing of glacial and paraglacial sedimentation in a monsoonal-influenced high Himalayan environment, the upper Bhagirathi Valley, Garhwal Himalaya: Sedimentary Geology, p. 1649–1656.

Benn, D.I., and Evans, D.J.A., 1998, Glaciers and glaciation: London, Arnold, 734 p.

Benn, D.I., and Lehmkuhl, F., 2000, Mass balance and equilibrium-line altitudes of glaciers in high mountain environments: Quaternary International, v. 65/66, p. 15–30.

Benn, D., and Owen, L.A., 1998, The role of the Indian summer monsoon and the mid-latitude westerlies in Himalayan glaciation: Review and speculative discussion: Journal of the Geological Society, v. 155, p. 353–363.

Benn, D.I., and Owen, L.A., 2002, Himalayan glacial sedimentary environments: A framework for reconstructing and dating the former extent of glaciers in high mountains: Quaternary International, v. 97–98, p. 3–26.

Benn, D.I., Kirkbride, M.P., Owen, L.A., and Brazier, V., 2003, Glaciated valley landsystems, *in* Evans, D.J., ed., Glacial landsystems: London, Edward Arnold, p. 372–406.

Bottino, G., Chiarle, M., Joly, A., and Mortara, G., 2002, Modelling rock avalanches and their relation to permafrost degradation in glacial environments: Permafrost and Periglacial Proceedings, v. 13, p. 283–288.

Bouchon, M., and Vallée, M., 2003, Observation of Long Supershear Rupture during the magnitude 8.1 Kunlunshan Earthquake: Science, v. 301, p. 824–826.

Chatellus, de.A., 1973, Le tremblement de terre du Pérou en 1970 dans la Cordillera Blanca: La Montagne et alpinisme: Paris, Club Aplin Français, v. 2, p. 67–72.

Dang, G., and Wang, Z., 2002, Characteristics of the surface rupture zone and main seismic hazards caused by the Ms 8.1 earthquake west of the Kunlun Pass, China: Constraints on the regional stability of the Qinghai-Tibet Plateau: Geological Bulletin Of China, v. 21, p. 105–108.

Derbyshire, E., 1981, Glacier regime and glacial sediment facies: A hypothetical framework for the Qinghai-Xizang Plateau, *in* Proceedings of Symposium on Qinghai-Xizang (Tibet) Plateau, Volume 2—Geological and Ecological Studies of Qinghai-Xizang Plateau: Beijing, China, Science Press.

Erismann, T.H., and Abele, G., 2001, Dynamics of rockslide and rockfalls: New York, Springer, p. 316.

Evans, D.J.A., and Fisher, T.G., 1987, Evidence of a periodic ice-cliff avalanche on north-west Ellesmere Island, N.W.T., Canadian high Arctic: Journal of Glaciology, v. 33, p. 68–71.

Fort, M., 2000, Glaciers and mass wasting processes: their influence on the shaping of the Kali Gandaki valley (higher Himalaya of Nepal): Quaternary International, v. 65/66, p. 101–119.

Fort, M., and Peulvast, J.-P., 1995, Catastrophic mass movements and morphogenesis in the peri-Tibetan ranges: Examples from west Kunlun, east Pamir and Ladakh, *in* Slaymaker, O., ed., Steepland geomorphology: New York, Wiley, p. 171–198.

Harvard, 2001, CMT online catalog: http://www.seismology.harvard.edu/.

Hewitt, K., 2002, Styles of rock-avalanche depositional complexes conditioned by very rugged terrain, Karakoram Himalaya, Pakistan, *in* Evans, S.G., and Degraff, J.V., eds., Catastrophic landslides: Effects, occurrence, and mechanisms: Geological Society of America Reviews in Engineering Geology, v. 15, p. 165–190.

Heybrock, W., 1935, Earthquakes as a cause of glacier avalanches in the Caucasus: Geographical Review, v. 25, p. 423–429.

Johnson, A.M., and Rodine, J.R., 1984, Debris flow, *in* Brunsden, D., and Prior, D.B., eds., Slope instability: Chichester, Wiley, p. 257–361.

Kääb, A., Wessels, R., Haeberli, W., Huggel, C., Kargel, J.S., and Khalsa, S.J.S., 2003, Rapid ASTER imaging facilitates timely assessment of glacier hazards and disasters: Eos (Transactions, American Geophysical Union), v. 84, p. 117 and 121.

Kidd, W.S.F., and Molnar, P., 1988, Quaternary and active faulting observed on the 1985 Academia Sinica–Royal Society geotraverse of Tibet: Philosophical Transactions of the Royal Society of London, v. 327, p. 337–363.

Kikuchi, M., and Yamanaka, Y., 2001, Special event page 2001/11/14 Qinghai Xinjiang Border, China (Mw 7.9): Tokyo, Earthquake Research Institute, http://wwweic.eri.u-tokyo.ac.jp/topics/200111140926/index.html.

Le Pichon, A., Guilbert, J., Vallée, M., Dessa, J.X., and Ulziibat, M., 2003, Infrasonic imaging of the Kunlun Mountains for the great 2001 China earthquake: Geophysical Research Letters, v. 30, ASC 9, p. 1–4.

Lehmkuhl, F., Owen, L.A., and Derbyshire, E., 1998, Late Quaternary glacial history of Northeastern Tibet: Quaternary Proceedings, v. 6, p. 121–142.

Li, H., Qi., X., Zhu, Y., Yang, J., Klinger, Y., Tapponnier, P., and Van der Woerd, J., 2003, Coseismic ruptures of the 14/11/2001, Mw = 7.8 Kokoxili earthquake near Hongsui Gou: European Union of Geosciences–American Geophysical Union–European Union of Geosciences Joint Assembly, Geophysical Research Abstract, v. 5, p. 8985.

Lin, A., Fu, B., Guo, J., Zeng, Q., Dang, G., He, W., and Zhao, Y., 2002, Co-seismic strike-slip and rupture length produced by the 2001 Ms 8.1 central Kunlun earthquake: Science, v. 296, p. 2015–2017.

Lliboutry, L.N., 1971, Les catastrophes glaciaires: La Recherche, v. 2, p. 417–425.

McSaveney, M.J., 1978, Sherman Glacier rock avalanche, Alaska, USA, *in* Voight, B., ed., Rockslides and avalanches: New York, Elsevier Scientific Press, p. 197–258.

Mériaux, A.-S., Klinger, Y., Li, H., Tapponnier, P., and Lacassin, R., 2001, Kokoxili Earthquake—Kunlun Fault (Tibet) 14 November 2001—Mw 7.9: Paris, Institut de Physique de Globe de Paris.

Owen, L.A., 1991, Mass movement deposits in the Karakoram Mountains: Their sedimentary characteristics, recognition and role in Karakoram landform evolution: Zeitschrift für Geomorphologie, v. 35, p. 401–424.

Perla, R.I., 1980, Avalanche release, motion and impact, *in* Colbeck, S.C., ed., Dynamics of snow and ice masses: New York, Academic Press, p. 397–462.

Plafker, G., and Ericksen, G.E., 1978, Nevados Huascaran avalanches, Peru, *in* Voight, B., ed., Rockslides and avalanches: New York, Elsevier Scientific Press, p. 277–314.

Rapp, A., 1959, Avalanche boulder tongues in Lappland; descriptions of little-known forms of periglacial debris accumulations: Geografiska Annaler, v. 41, p. 34–48.

Richardson, S.D., and Reynolds, J.M., 2000, An overview of glacial hazards in the Himalayas: Quaternary International, v. 65/66, p. 31–47.

Rivera, L., Van der Woerd, J., Tocheport, A., Klinger, Y., and Lasserre, C., 2003, The Kokoxili, November 14, 2001, earthquake: History and geometry of the rupture from teleseismic data and field observations: EGS-AGU-EUG Joint Assembly, Geophysical Research Abstract, v. 5, p. 10910.

Rothlisberger, H., 1977, Ice avalanches: Journal of Glaciology, v. 19, p. 669–671.

Rouse, W.C., 1984, Flowslides, *in* Brunsden, D., and Prior, D.B., eds., Slope instability: Chichester, Wiley, p. 491–522.

Rüegg, W., 1962, La Cordillère Blanche de Pérou et la catastrophe du Huascaran: Die Alpen, v. 38, p. 275–280.

Scheiwiiler, T., and Hutter, K., 1982, Lawinendynamik, Übersicht über experimente und theoretische modelle von fliess und Staublawinen: Mitteilung der Versuchsanstalt für Wasserbau, Hydrologie und Glaziologie an der Eidgenössischen Technischen Hochschule (Zürich), v. 58.

Su, Z., and Shi, Y., 2002, Response of monsoonal temperate glaciers to global warming since the Little Ice Age: Quaternary International, v. 97/98, p. 123–131.

Tufnell, L., 1984, Glacier hazards: Harlow, Longman Group Ltd., p. 97.

van der Woerd, J., Ryerson, F.J., Tapponnier, P., Mériaux, A.-S., Gaudemer, Y., Meyer, B., Finkel, R.C., Caffee, M.W., Zhao, G., and Xu, Z., 1998, Holocene left-slip rate determined by cosmogenic surface dating on the Xidatan segment of the Kunlun fault (Qinghai, China): Geology, v. 26, p. 695–698.

van der Woerd, J., Ryerson, F.J., Tapponnier, P., Mériaux, A.-S., Gaudemer, Y., Meyer, B., Finkel, R.C., Caffee, M.W., Zhao, G., and Xu, Z., 2000, Uniform slip-rate along the Kunlun fault: Implications for seismic behaviour and large-scale tectonics: Geophysical Research Letters, v. 27, p. 2353–2356.

van der Woerd, J., Meriaux, A.-S., Klinger, Y., Ryerson, F.J., Gaudemer, Y., and Tapponnier, P., 2002a, The 14 November 2001, M_w = 7.8 Kokoxili earthquake in northern Tibet (Qinghai Province, China): Seismological Research Letters, v. 73, p. 125–135.

van der Woerd, J., Ryerson, F.J., Tapponnier, P., Meriaux, A.-S., Meyer, B., Gaudemer, Y., Finkel, R.C., Caffee, M.W., Guoguang, Z., and Zhiqin, X., 2002b, Uniform post-glacial slip-rate along the central 600 km of the Kunlun fault (Tibet), from ^{26}Al, ^{10}Be and ^{14}C dating of riser offsets, and climatic origin of the regional morphology: Geophysical Journal International, v. 148, p. 356–388.

van der Woerd, J., Klinger, Y., Tapponnier, P., Xu, X., Chen, W., Ma, W., and King, G., 2003, Coseismic offsets and style of surface ruptures of the 14 November 2001 Mw = 7.8 Kokoxili earthquake (northern Tibet): European Union of Geosciences–American Geophysical Union–European Union of Geosciences Joint Assembly, Geophysical Research Abstract, v. 5, p. 11151.

Vivian, R., 1979, Les glaciers sont vivants: Paris, Denoël, p. 238.

Wang, W., 1987a, Existing glaciers and their variation in the northeastern part of the Qinghai-Xizang Plateau, *in* Hovermann, J., and Wang, W., eds., Reports on the Northeastern part of the Qinghai-Xizang (Tibet) plateau: Beijing, Science Press, p. 22–45.

Wang, J., 1987b, Climatic Geomorphology of the Northeastern part of the Qinghai-Xizang Plateau, *in* Hovermann, J., and Wang, W., eds., Reports on the Northeastern part of the Qinghai-Xizang (Tibet) Plateau: Beijing, Science Press, p. 140–175.

Wieczorek, G.F., 2002, Catastrophic rockfalls and rockslides in the Sierra Nevada, USA, *in* Evans, S.G., and Degraff, J.V., eds., Catastrophic landslides: Effects, occurrence, and mechanisms: Geological Society of America Reviews in Engineering Geology, v. 15, p. 165–190.

Xu, X., Chen, W., Yu, G., Ma, W., Dai, H., Zhang, Z., Chen, Y., He, W., Wang, Z., and Dang, G., 2002a, Characteristic features of the surface ruptures of the Hoh Sai Hu (Kunlun Shan) earthquake (Ms 8.1), northern Tibetan plateau, China: Seismology and Geology, v. 24, p. 1–13.

Xu, X., Chen, W., Ma, W., Yu, G., and Chen, G., 2002b, Surface rupture of the Kunlunshan earthquake (Ms 8.1), northern Tibetan plateau, China: Seismological Research Letters, v. 73, p. 884–892.

Xu, X., Chen, W., Ma, W., Van der Woerd, J., Klinger, Y., Tapponnier, P., King, G., Zhao, R., and Li, J., 2003, Re-evaluation of co-seismic strike-slip and surface rupture length of the 2001 Kunlunshan earthquake, northern Tibetan plateau: European Union of Geosciences–American Geophysical Union–European Union of Geosciences Joint Assembly, Geophysical Research Abstract, v. 5, p. 3870.

MANUSCRIPT RECEIVED BY THE SOCIETY 8 JANUARY 2003
REVISED MANUSCRIPT RECEIVED 22 MAY 2003
MANUSCRIPT ACCEPTED 23 JUNE 2003

Printed in the USA